Algerian Journal of Engineering Research 03-2 (2019) 45-51

Numerical Study of Natural Convection in a Closed Cavity

Zermane Samah[1], Boulkroune Nadjet, Bouneb Nardjess

Laboratoire de l'ingénierie des procédés de l'environnement, Université Constantine 3, Constantine, Algérie, Fax : 00213.31.84.63.04, [1]zermanesamah@yahoo.fr

Abstract

The present work concerns a numerical study on natural convection in a square cavity heated from the base wall while the upper wall was adiabatic and the vertical walls were maintained at a constant cold temperature. The equations governing the phenomenon were described using the stream function ψ and the vorticity ω. They were expressed in terms of dimensionless parameters and after a finite differences discretization the obtained system of algebric equations was solved using the scanning method and the Thomas algorithm for the temperature and the vorticity, and an iterative process (NLOR) for the stream function. A computing code in Fortran was developed to perform the required calculations to obtain the fluid behaviour inside the square cavity.

Keywords: *Natural convection, NLOR, Square cavity, Finite differences*

I. INTRODUCTION

Any transformation of energy is carried out according to the second principle of thermodynamics and takes into account a certain degree of degradation with heat as the most degraded form due to the important disorder, and is mostly encountered in all natural or industrial processes. The heat transmission had been the base of many sensitive technologies like those dealing with Nuclear, Solar, Aerospace, etc. and this since the development of Fourier's law in 1811. Its development was also enhanced by various energy crises through which had gone the world in the past. Heat is transfered under different modes mainly forced and natural convection which is the main concern of the present study, particularly in cavities.

In fact natural convection is widely considered in the literature. A study of this phenomenon was reported in R. Delahaye (2002) [1] with a binary fluid layer filling a horizontal rectangular cavity with adiabatic vertical walls, assuming that all the boundaries of the cavity were rigid and impermeable, excepted the undeformable free upper surface. A numerical study was reported in [2] and considered the phenomenon of laminar mixed convection in a ventilated cavity the left vertical wall of which was subject to a constant temperature higher than the ambient one while the other wall were considered as adiabatic. Numerical simulations based on the resolution of the governing equations were performed for cases considering two Grashof number and four Richardson number values. The study of the temporal variation of the mean Nusselt number was presented for the different values of the two dimensionless numbers and the analysis of the obtained results highlighted single and multi-cell flow for the different considered cases. A study of natural convection in closed cavities was reported in considering the effect of Prandtl and Rayleigh numbers on the flow, and this for different boundary conditions. The variations of the local numbers were also presented in [4] through a numerical study of the two-dimensional laminar natural convection of a Newtonian fluid (air) confined in an elongated rectangular enclosure of square cross section. It was heated from below and the other three walls are kept at the same cold temperature. The governing equations were written in formulation "function of stream-vorticity" and integrated using a finite difference method. A numerical simulation of laminar mixed convection in a square cavity with several inputs was considered in [5] with the left vertical wall subject to a constant uniform temperature, while the other walls were kept adiabatic. The governing equations described the phenomenon still using the formulation "stream function ψ and vorticity ω". A digital simulation of natural convection in a rectangular enclosure filled with liquid metal and subject to a horizontal temperature gradient was carried out in [6]. A

modeling of the problem in 2D and 3D was carried out using a code which was based on the finite element method. A numerical study on two-dimensional natural convection in a square and inclined porous material was proposed in [7]. Mixed convection in a square cavity with cold and mobile side walls was considered in [8] with a heat source placed in the middle of the upper wall and the other walls were assumed to be adiabatic. A numerical study of laminar natural convection in a square enclosure with partial heating of the lower wall and cooling of the side walls was carried out in [9] to simulate the case of accidental heat generation due to a fire in a building for a nuclear reactor or in an assembly cabin for electronic components.

A numerical two-dimensional heat transfer through slabs used for the construction of building ceilings was considered and the equations which governed the conductive, convective and radiative heat transfer were discretized by the control volumes method and were solved by the SIMPLE algorithm [10].

II. MATHEMATICAL FORMULATION

A square cavity of dimension L × L was considered as shown in Figure 1.

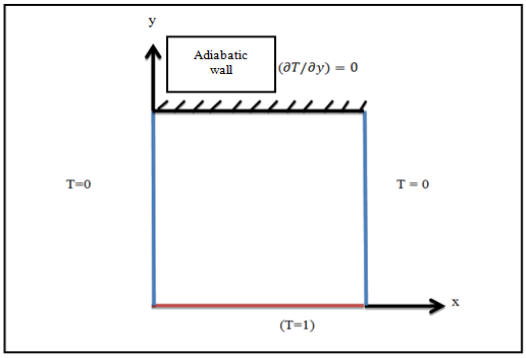

Figure 1 . Considered configuration

The base horizontal was subject to a constant temperature equal to 1 and the opposite wall was adiabatic and the temperatures of the vertical surfaces were zero.

The flow governing equations are based on the Mass (continuity), Energy, and Momentum conservation equations are respectively expressed as follows:

$$\frac{\partial u}{\partial x}+\frac{\partial v}{\partial y}=0 \qquad (1)$$

$$u\frac{\partial u}{\partial x}+v\frac{\partial u}{\partial y}=-\frac{1}{\rho}\frac{\partial p}{\partial x}+\nu\left(\frac{\partial^2 u}{\partial x^2}+\frac{\partial^2 u}{\partial y^2}\right) \qquad (2)$$

$$u\frac{\partial v}{\partial x}+v\frac{\partial v}{\partial y}=-\frac{1}{\rho}\frac{\partial p}{\partial y}+\nu\left(\frac{\partial^2 v}{\partial x^2}+\frac{\partial^2 v}{\partial y^2}\right)+g\beta\,(T-T_C) \qquad (3)$$

$$u\frac{\partial T}{\partial x}+v\frac{\partial T}{\partial y}=\alpha\left(\frac{\partial^2 T}{\partial x^2}+\frac{\partial^2 T}{\partial y^2}\right) \qquad (4)$$

In order to be independent on the actual dimensions and properties, the equations were written in terms of the following dimensionless variables:

$$X=\frac{x}{L}\ ,\quad Y=\frac{y}{L}\ ,\quad U=\frac{uL}{\alpha}\ ,\quad V=\frac{vL}{\alpha}\ ,\quad \theta=\frac{T-T_c}{T_{h-}T_c}\ ,\quad P=\frac{pL^2}{\rho\alpha^2}$$

The introduction of the previous dimensionless variables into the differential equations (1), (2), (3), (4), in addition to the two numbers Pr, Ra; results in the following dimensionless mathematical model:

$$\frac{\partial U}{\partial X}+\frac{\partial V}{\partial Y}=0 \qquad (5)$$

$$U\frac{\partial U}{\partial X}+V\frac{\partial U}{\partial Y}=-\frac{\partial P}{\partial X}+\Pr\left(\frac{\partial^2 U}{\partial X^2}+\frac{\partial^2 U}{\partial Y^2}\right) \qquad (6)$$

$$U\frac{\partial V}{\partial X}+V\frac{\partial V}{\partial Y}=-\frac{\partial P}{\partial Y}+\Pr\left(\frac{\partial^2 V}{\partial X^2}+\frac{\partial^2 V}{\partial Y^2}\right)+\mathrm{Ra}\,\Pr\,\theta \qquad (7)$$

$$U\frac{\partial \theta}{\partial X}+V\frac{\partial \theta}{\partial Y}=\frac{\partial^2 \theta}{\partial X^2}+\frac{\partial^2 \theta}{\partial Y^2} \qquad (8)$$

By differentiating Equation (6) with respect to Y and Equation (7) with respect to X and then by subtracting the two equations obtained, gives:

$$\frac{\partial U}{\partial X}\left(\frac{\partial U}{\partial Y}-\frac{\partial V}{\partial X}\right)+U\frac{\partial}{\partial X}\left(\frac{\partial U}{\partial Y}-\frac{\partial V}{\partial X}\right)+\frac{\partial V}{\partial Y}\left(\frac{\partial U}{\partial Y}-\frac{\partial V}{\partial X}\right)+V\frac{\partial}{\partial Y}\left(\frac{\partial U}{\partial Y}-\frac{\partial V}{\partial X}\right)=\Pr\left[\frac{\partial^2}{\partial X^2}\left(\frac{\partial U}{\partial Y}-\frac{\partial V}{\partial X}\right)+\frac{\partial^2}{\partial Y^2}\left(\frac{\partial U}{\partial Y}-\frac{\partial V}{\partial X}\right)\right]-\mathrm{Ra}\,\Pr\frac{\partial \theta}{\partial X} \qquad (9)$$

By definition the vorticity is given as [11]:

$$\omega=\frac{\partial U}{\partial Y}-\frac{\partial V}{\partial X} \qquad (10)$$

Equation (9) becomes:

$$U\frac{\partial \omega}{\partial X}+V\frac{\partial \omega}{\partial Y}=\Pr\left(\frac{\partial^2 \omega}{\partial X^2}+\frac{\partial^2 \omega}{\partial Y^2}\right)-\mathrm{Ra}\,\Pr\frac{\partial \theta}{\partial X} \qquad (11)$$

By definition the velocity vectors are given by [11]:

$$U = \frac{\partial \psi}{\partial Y} \quad , \quad V = -\frac{\partial \psi}{\partial X} \tag{12}$$

Replacing U and V in Equation (10) gives:

$$\frac{\partial^2 \psi}{\partial Y^2} + \frac{\partial^2 \psi}{\partial X^2} = \omega \tag{13}$$

III. Heat transfer Coefficient

The interest is in the heat transfer at the level of the heated wall and is expressed by the local Nusselt number as:

$$Nu_x = -\left|\frac{\partial T}{\partial X}\right|_{Y=0} \tag{14}$$

The value of the average Nusselt number along the heated wall is given as:

$$Nu = \frac{h\,H}{k} = \int_0^1 -\left(\frac{\partial T}{\partial X}\right)_{Y=0} dX \tag{15}$$

Where h represents the average coefficient of heat transfer

IV. Boundary Conditions

The resolution of the system of equations obtained previously requires the boundary conditions values for each independent variable.

$$Y = 0, \quad 0 \le X \le 1, \quad \theta = 1 \quad \text{and}$$

$$Y = 1, \quad 0 \le X \le 1, \quad \frac{\partial \theta}{\partial Y} = 0 \tag{16}$$

$$X = 0, \quad 0 \le Y \le 1, \quad \theta = 0 \quad \text{and}$$

$$X = 1, \quad 0 \le Y \le 1, \quad \theta = 0 \tag{17}$$

The conditions of the vorticity are identical on all the walls, and can be noted as follows:

$$\omega = \omega_p \tag{18}$$

With

$$\omega_p = \frac{2\,(\psi_p - \psi_{p+1})}{\Delta \eta^2} \tag{19}$$

This is obtained from a first order discretization with p denoting the wall and Δη the space step in the normal direction.

V. Numerical Formulation

The finite difference method for the discretization of the differential equations was used for a two-dimensional numerical resolution of Mass, Momentum and Energy conservation equations. The solution was implemented to simulate the circulation of air and the temperature field in the enclosure. The resolution was carried out by means of a FORTRAN computing code, basing also on the scanning method.

VI. Results and discussion

A. Choice of mesh steps (ΔX, ΔY)

The setting of the mesh step values is an important factor upon which depends the precision of the numerical results. In order to minimize the influence of this mesh on the solution, several simulations were performed by comparing the values of the mean Nusselt number. The results obtained are given in Table 1, with:

i: representing the total number of nodes in the horizontal direction (OX).

m: representing the total number of nodes in the horizontal direction (OY).

$$\text{Error} = \left|\frac{Nu_m(70\times70) - Nu_m(i\times m)}{Nu_m(i\times m)}\right| \times 100 \tag{20}$$

The Nusselt number for a mesh of (70 × 70) was taken as a reference for the calculation of the error expressed as a percentage. According to the results, a mesh of (50 × 50) was adopted.

Table 1 . Comparison of the average Nusselt number for different mesh.

i× m	Nu_{Av}	Error (%)
50×50	5.483370	26.473860%
30×30	3.659899	50.924660%
70×70	7.457715	-

B. Validation of Fortran code

In [3] a closed square cavity was considered with the two vertical walls kept cold while the upper wall was adiabatic, and the lower wall is warm. The computing code was used for this case, calculating the heat transfer coefficient. The obtained results were compared with the reported values as shown in Table 2, for different values of

Prandtl (0.7, 10) and of the Rayleigh (10^3) numbers. The error was around 5.17% for a Rayleigh number of 10^3 and a Prandtl number of (0.7 and even 10).

Table 2 . Comparison of the heat transfer coefficient between the present work and [3]

	Nu_{av}	
	Rayleigh number Ra = 10^3	
Prandtl number	Pr = 0.7	Pr = 10
From **[3]**	5.2	5.2
This work	5.483370	5.483370
Error (%)	5.167807	5.167807

C. Results and discussion

C.1 Stream function

Figures 2 and 3 show the stream functions in steady state and in two dimensions x and y, for Rayleigh numbers of 10^3 and 10^5, and Prandtl numbers 0.7 and 10. It is noted that generally in steady state the stream functions represent two almost symmetrical cells for all the studied cases inside the cavity.

On the other hand there was a negligible influence of the number of Prandtl (by comparing the right and left figures) showing the nature of the flow by natural convection whatever the number of Prandtl. However comparatively to Rayleigh number as shown in Figures 2 and 3, a remarkable decrease was noted in the case of Ra = 10^5, relatively to the cell on the right.

So the structure of the flow presented notable differences only for a number of Ra = 10^5 where an influence of this number to lead the regime to a forced convection, was found.

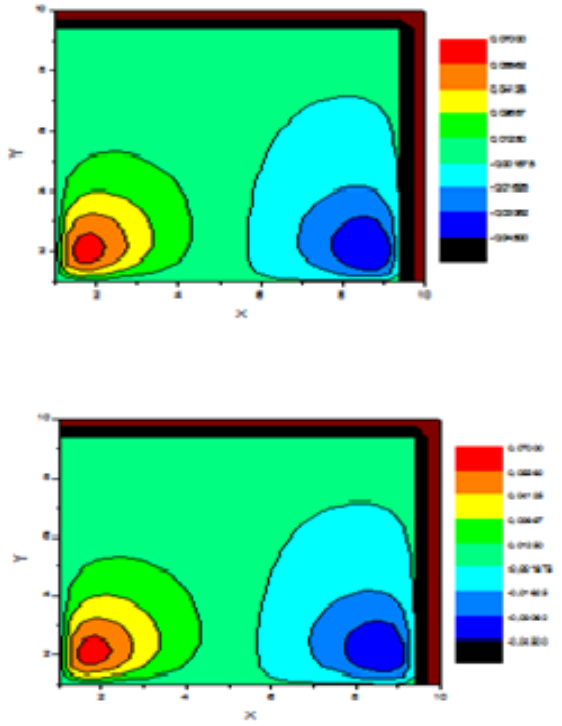

Figure 2 . Current functions Ra=10^3 (a) Pr=0.7 (b) Pr=10

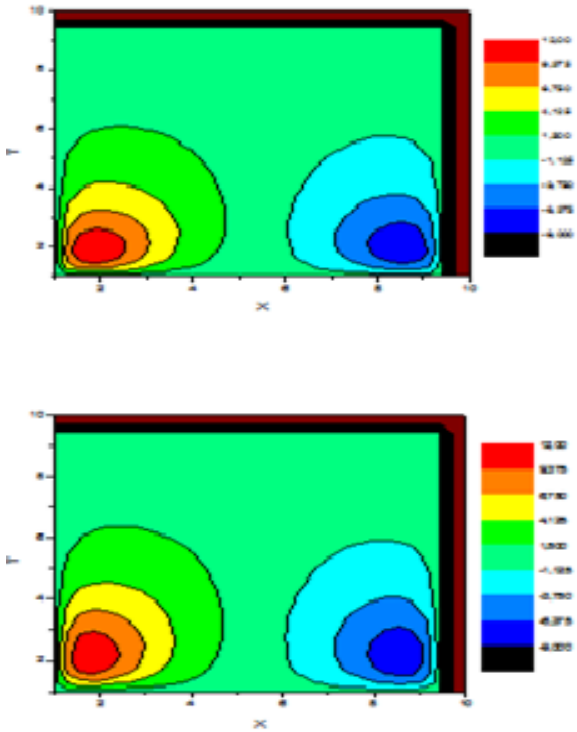

Figure 3 . Current functions Ra=10^5 (a) Pr=0.7 (b) Pr=10

C.2 Isotherms

Figures 4 and 5 represent steady state isotherms in two dimensions x and y, Rayleigh numbers of 10^3

and 10^5, and again for the two Prandtl numbers of 0.7 and 10.

It is observed that the isotherms represented in stationary regime an almost linear evolution from the lower hot wall for all the cases studied inside the cavity.

On the other hand it was also noted that there was a negligible influence of the Prandtl number but still remarkable compared to the Rayleigh number (by comparing Figures 4 and 5), particularly with respect to the cell structure of the evolution of the temperature in the case of Ra = 10^5. So the distribution of the temperature was linear for a low Ra, and a high temperature gradient of in the vicinity of the isothermal faces was observed when Ra increased. It was also observed that the thermal boundary layer developed over about 20% of the cavity when Ra = 10^3 and about 25% of the cavity for uniform heating when Ra = 10^5.

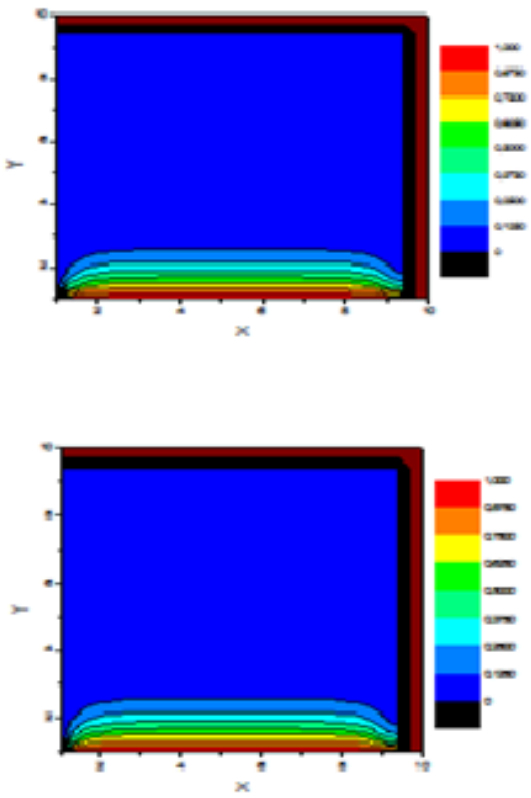

Figure 4 . Isotherms Ra=10^3
(a) Pr=0.7 (b) Pr=10

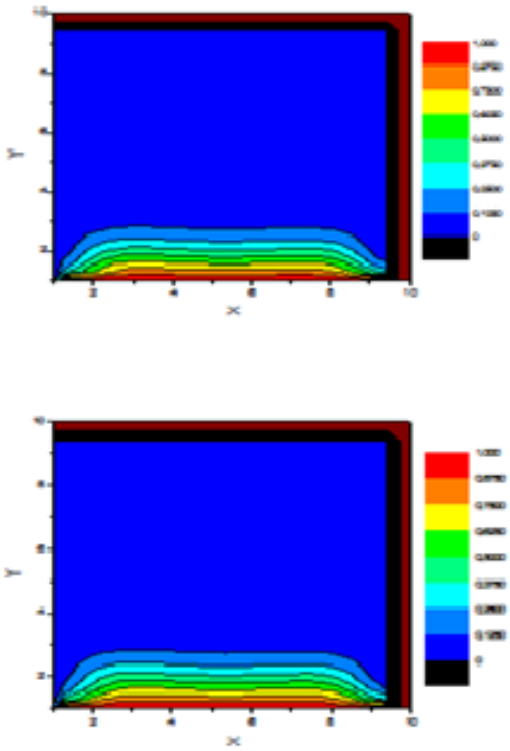

Figure 5 . Isotherms Ra=10^5
(a) Pr=0.7 (b) Pr=10

C.3 Profils of vertical velocity

Figures 6 and 7 represented in steady state the variation of the velocity V as a function of X and this for the Rayleigh numbers 10^3 and 10^5, and again for the two numbers of Prandtl 0.7 and 10.

It was noticed that the velocities for Ra = 10^3 shown in Figure 6 decreased then increased but in a very small part (from X = 0 to X = 0.03), then they stabilized until reaching X = 0.9 where they again decreased then increased almost in the same way. It is noted that the negative velocities in the station Y = 0.1 were more important than those of Y = 0.5 then Y = 0.8.

This can be explained by the importance of the recirculation zones at the inlet and then in the middle and finally at the outlet of the cavity. On the other hand a comparison of the profiles of the component V between shown in Figure (a) and (b) where the number of Pr increased from 0.7 to 10, showed that there was not a great influence on velocity profiles.

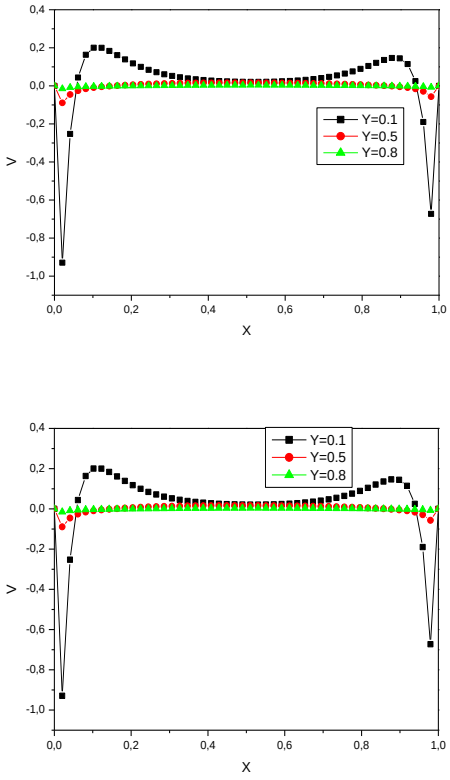

Figure 6. Profil of vertical velocity , (a) Pr=0.7, (b) Pr=10

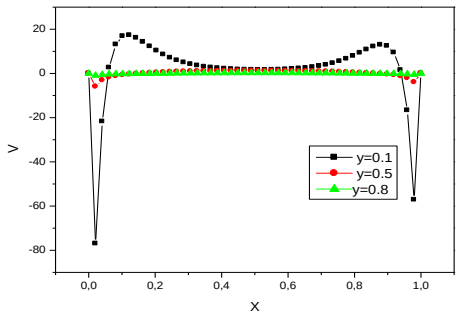

(a)

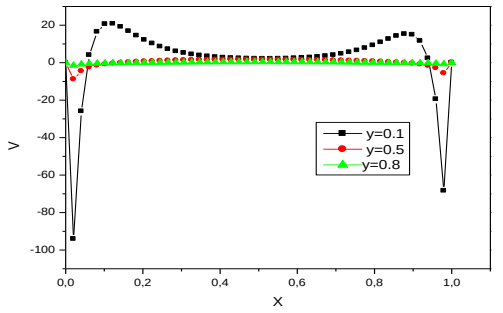

(b)

Figure 7 . Profil of vertical velocity Ra=10^5, (a) Pr=0.7, (b) Pr= 10

C.4 Profils of horizontal velocity

Figures 8 and 9 represented in stationary regime the variation of the velocity U as a function of Y and this for the Rayleigh numbers of 10^3 and 10^5, and again for the two Prandtl numbers 0.7 and 10. It was noticed that generally the velocity U was positive, then negative and finally vanished in the area of x = 0.1 (cavity entry) and that U was zero in the middle of the cavity, and finally it was negative, then positive and finally cancelled for x = 0.8 (cavity output)

All these can be explained by the way of circulation of the fluid inside the cavity. Therefore the fluid was set in motion under the sole effect of the differences in densities resulting from the differences in temperatures on the borders.

On the other hand it was noticed that there was a negligible influence of the Prandtl number (by comparing the figures on the right and on the left) but remarkable compared to the Rayleigh number (by comparing the figures 8 and 9) especially compared to the maximum values of U where they reached the values of 25 and 60 in the case of Rayleigh equal to 10^3 and 10^5, respectively.

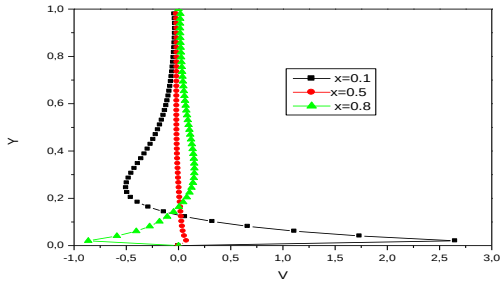

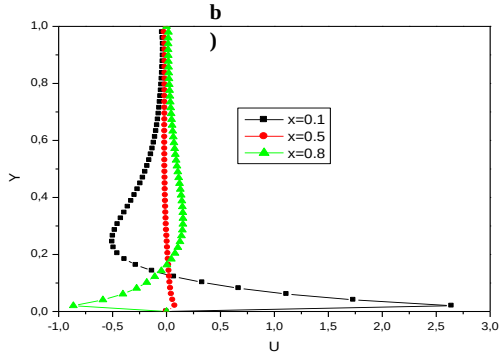

Figure 8 . Profil of horizontal velocity Ra=10^3 (a) Pr=0.7, (b) Pr= 10

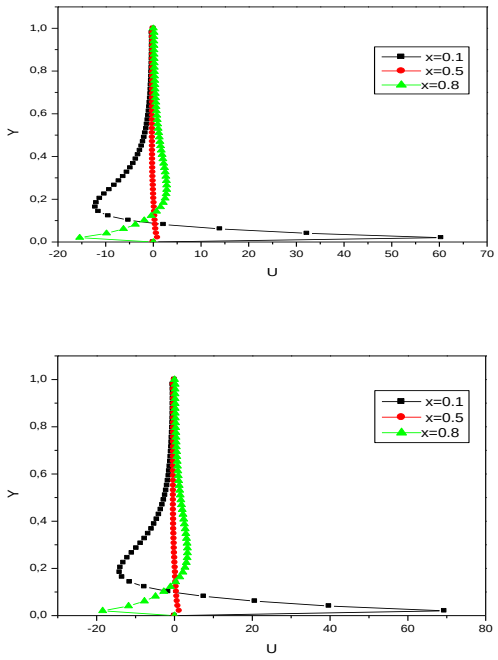

Figure 9 . Profil of horizontal velocity, Ra=10^5 (a) Pr=0.7, (b) Pr= 10

Conclusion

The results showed that beyond a Prandtl number (0.7 to 10) for the case considered) the distribution of isotherms and stream lines in the studied cavity, remained practically unchanged, compared to the appearance of zones of contrarotative recirculation in the lower part of the cavity on the one hand, and the distribution of the temperature of the fluid along the lower hot wall on the other hand which showed the nature of the flow by natural convection whatever the number of Pr. The results were also presented in the form of hydrodynamic fields for different values of Rayleigh numbers. The flow structure only showed notable differences for a number of Ra = 10^5 where an influence of this number was found to lead the regime towards a forced convection. It was observed that the thermal boundary layer developed over about 20% of the cavity when Ra = 10^3 and about 25% of the cavity for uniform heating when Ra = 10^5

List of symbols:

Cp	Specific heat at constant pressure	J/Kg.K
h	Coefficient of heat transfer	W/m².K
k	Conductivity	W/m.K
Nu	Average Nusselt number	-
Nu_X	Local Nusselt number	-
p	Pression	Pa
Pr	Prandtl number , ν/α	-
Ra	Rayleigh number , $g\,\beta(T_h - T_c)L^3Pr/\nu$	-
T	Temperature	K
T_c	Cold Temperature	K
T_h	Hot Temperature	K
u	Velocity	m/s
α	Diffusivity, $K/\rho\, c_p$	m^2/s
ν	Cinematic Viscosity	m^2/s
ρ	Volumic mass	g/m^3

References

[1] R.Delahaye, Influence de l'effet Soret sur la convection au sein d'une couche de fluide binaire, Projet de Maîtrise Cours, École Polytechnique de Montréal, 2002.

[2] S.Zermane, Etude numérique de la convection mixte laminaire dans des cavités ventilées, mémoire de Magister, Université Mentouri de Constantine 2004.

[3] T.Basak et al, Effects of thermal boundary conditions on natural convection flows within a square cavity, International Journal of Heat and Mass Transfer 49, (2006) 4525–4535.

[4] F. P. Kiéno, A.Ouédraogo et M.Daguenet, Etude de la convection naturelle dans une cavité allongée horizontale, J. Soc. Ouest-Afr. Chim. 024 ; (2007), 21 - 34.

[5] M.Belhi, , Etude Numérique de la Convection Naturelle dans une Cavité Ayant Plusieurs Entrées, mémoire de Magister, Université Mentouri de Constantine, 2007.

[6] N.Ibrir et S. Rahal, Simulation numérique en 3D de la convection naturelle dans les fluides à bas nombres de Prandtl, Revue Des Energies Renouvelables CISM'08 Oum El Bouaghi, (2008), 183-194.

[7] A.Latreche, Etude numérique de la convection naturelle en milieux poreux saturé de fluide dans une cavité carrée à orientation variable, mémoire de Magister, Université Mentouri de Constantine, 2010.

[8] H.Benhacine, Etude de l'écoulement conductif d'un fluide dans une cavité, mémoire de magister, Université Mentouri de Constantine, 2010.

[9] M.Guestal, Modélisation de la Convection Naturelle Laminaire dans Une Enceinte Avec Une Paroi Chauffée Partiellement, mémoire de Magister, Université Mentouri de Constantine, 2010.

[10] T.Ait-Taleb, A.Abdelbaki et Z.Zrikem, Transferts thermiques couplés dans les planchers alvéolaires chauffés par le haut, Revue de Mécanique Appliquée et Théorique, Vol. 2, 3 , (2010) 275-284.

[11] J.Wiley, Applied numerical methods, 1969.